ENERGY OPTIMIZATION TO REPLACE R134A IN A VAPOR COMPRESSION REFRIGERATION CYCLE

Thiago Pereira Silva
Kássio Nogueira Cançado
Katrine Barbosa Oliveira Chaves
Ramon de Paoli Mendes
Luiz Machado
Graduate Program in Energy Engineering – Federal Center for Technological Education of Minas Gerais – Av. Amazonas, 7675 – Nova Gameleira, Belo Horizonte – MG, 30510-000
tiagok8cefet@hotmail.com
cancado@hotmail.com
katrine@ufmg.br
ramondepaoli@yahoo.com
luizm@demec.ufmg.br

Abstract. With the new directive implemented in 2014 by the European Parliament with the objective of reducing the use of gases with high GWP potential in the European Union and the growing increase in the refrigeration and air conditioning markets, several studies have been carried out with the objective of improving the efficiency of these cycles and find efficient alternatives to replace R134a as a refrigerant. The present work created a mathematical model capable of simulating different operating conditions of a refrigeration cycle that was validated with experimental data and enabled the use of a genetic-type optimization algorithm to maximize energy efficiency based on the choice of condensing pressure and refrigerant fluid. Adjusting the condensing pressure resulted in a 22% increase in the COP. COP increase of 32% with R134a being the most energy efficient fluid. For the replacement of R134a, the fluid that showed the highest energy efficiency was R152a with a COP increase of 28% in relation to the initial conditions and efficiency 5% lower than that presented by R134a. The results also showed that, if well adjusted, it is possible to retrofit a refrigeration system without loss of refrigeration capacity and energy efficiency.

Keywords*: Optimization, GWP, COP, Refrigeration Cycle, R134a*

1. INTRODUCTION

In 2014, Directive 517/2014 was introduced by the European Parliament to reduce the use of high GWP (Global Warming Potential) gases in the European zone in order to limit global climate change caused by these . These restrictions affect the vast majority of artificial soft drinks (SÁNCHEZ *et al*., 2017).

Mechanical vapor compression refrigeration (CRCV) cycles are widely used in industrial, residential and automotive applications for heating and cooling, as well as controlling other air properties such as humidity. The vast majority of these cycles use R134a as the working fluid, which is included in the restrictions imposed by the European Parliament due to its relatively high GWP index.

Thus, the significant increase in the fields of refrigeration and air conditioning, combined with the need to replace R134a with fluids with lower GWP, stimulate studies with the aim of increasing the efficiency of CRCV and identifying new alternatives for refrigerant fluids with low GWP.

In this scenario, it is possible to mention some fluids that, among other reasons, have been extensively studied to replace R134a due to two characteristics. The first is that having characteristics similar to those of R134a allows the replacement of the fluid to be done by the “Drop-in” or “retrofit” process, which consists of the direct replacement of the fluid, changing only when necessary the compressor lubricant or other changes. such as the expansion valve for example. The second characteristic is having the GWP index lower than 150, which is the limit stipulated by the new European guidelines. Five fluids were analyzed in this work: R134a itself (comparison basis); the R152a; the R1234yf; the R1234ze(E) and the R600a.

R134a is a hydrofluorocarbon that has a high GWP index (1500), which is why its use has been restricted (CABELLO *et al*., 2015), in addition to having low toxicity and not being flammable (ASHRAE A1 classification). R152a is a hydrofluorocarbon that has a low GWP number (138) and is ASHARE A@ rated for flammability, making it less safe than R134a. The use of R152a saw renewed interest due to its low GWP index and its similarity to R134a (CABELLO *et al*., 2015). In their work CABELLO *et al*., (2015) carried out an energy analysis replacing the R134a of a conventional vapor compression plant equipped with a hermetic compressor by the “Drop in” process. The results showed a gain in energy efficiency of 13% on the other hand, the cooling capacity decreased by 10%. BOLAJI (2010) carried out an experimental study to evaluate the energy efficiency of a domestic refrigerator replacing the R134a refrigerant with R152a and R32. The fluid was replaced by the "Drop in" process and the results showed that the use of R152a promoted a 4.7% COP increase while the replacement by R32 resulted in an 8.5% lower COP, thus concluding that R152a from the point of view of efficiency is better than R32 for all domestic refrigerator operating conditions.

R1234yf is a hydrofluorolefin (HFO) that has a GWP less than 1 and is considered slightly flammable (ASHRAE classification A2L). BELMAN-FLORES *et al*., (2017) carried out an experimental study with three identical domestic

refrigerators using R1234yf as an immediate substitute for R134a, for which an alternative methodology was proposed in order to estimate the ideal mass load for R1234yf. The use of such methodology presented an average (for the 3 refrigerators) of optimal load of 92.2 g, approximately 7.8% less than that of R134a, representing a 4% increase in energy consumption compared to R134a.

R1234ze(E) is a hydrofluorolefin (HFO) considered to be slightly flammable (ASHRAE classification A2L), thus encountering some resistance to its use. (MOTA-BABILONI *et al.*, 2016) SÁNCHEZ *et al.*, (2018) carried out experimental studies in a direct expansion refrigeration plant converted to an indirect expansion plant. The results were analyzed in terms of energy consumption for a medium temperature commercial refrigeration unit. The refrigerants used in the analysis were R134a for the direct system, and R134a, R152a and R1234ze (E) for the indirect system. The analysis of the results showed that the adoption of an indirect configuration resulted in an increase in the total energy consumption of the plant, regardless of the refrigerant adopted. The average increment recorded was 21.8% for R134a, 18.7% for R152a and finally 27.2% for R1234ze (E), with R1234ze(E) being lower than R152a from the point of view of energy efficiency.

R600a or isobutane has an insignificant GWP index, however its use encounters some resistance because it is considered flammable (ASHRAE classification A3). JOYBARI *et al*., (2013) performed an exergy analysis to investigate the performance of a domestic refrigerator originally manufactured to use 145 g of R134a. The results obtained showed that a load of 60g of R600a presented an energy efficiency similar to that of R134a. Subsequently, the analysis of values such as amount of R600a, condenser fan rotation and compressor power showed that the most significant parameter in the cycle performance is the R600a charge in the system, which is in the optimal condition of 50g. This value is 66% lower than R134a which not only brings economic advantages but also reduces the risk of flammability.

SÁNCHEZ *et al.*, (2017) carried out a study on the energy performance of fluids with low GWP as an alternative to R134a. In his work, a test bench was used to test different operating conditions for R134a and five other alternative fluids (R152a, R1234yf, R1234ze(E), R600a, R290). The analysis of the results showed that the refrigerants R152a and R1234yf are suitable for the replacement of R134a from the point of view of energy consumption and the cooling capacity of the cycle. The other fluids proved to be unsuitable for replacing R134a.

The present work proposes a new methodology to increase the efficiency of refrigeration cycles. For this, the work was divided into two parts with the objective of creating a mathematical model that allows simulating different operating conditions of a refrigeration cycle and using an optimization algorithm to find the operating point that presents the highest energy efficiency for the condition. simulated operation.

In the creation of the model, MatLab software and the CoolProp thermodynamic properties library were used. The model validation was performed using experimental data obtained by SÁNCHEZ *et al*., (2017). The optimization was carried out in two ways: The first used a non-linear programming algorithm to maximize the system COP, manipulating the condensing pressure; The second used a genetic-type algorithm to maximize the COP by manipulating the condensing pressure and the refrigerant fluid, in this way it is possible to determine which fluid and which operating point are ideal for a given condition.

2. MATERIALS AND METHODS

2.1 VAPOR COMPRESSION REFRIGERATION CYCLE

Figure 1 – Vapor compression refrigeration cycle

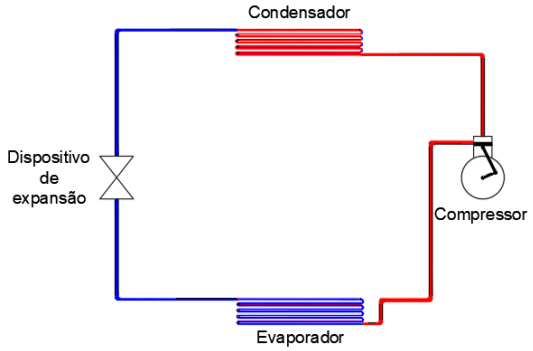

Source: Prepared by the author, 2022.

The basic scheme of a vapor compression refrigeration cycle consists of a working fluid that absorbs heat from one source and transfers it to another by changing the phase of the fluid within a closed circuit. The CRCV consists of 4 basic components: Compressor, condenser, expansion device and evaporator. The simulated heat exchangers are the same for the evaporator and condenser and are of the double tube type using water as the secondary fluid.

In the CRCV, the circulating refrigerant fluid enters the compressor as saturated or superheated vapor and is compressed to a higher pressure and temperature (Condensing Temperature and Pressure). The superheated steam travels

through the condenser, is cooled until it condenses, the heat being rejected to an external source. The liquid refrigerant now passes through an expansion device such as a valve or capillary tubes, suddenly decreasing the pressure, resulting in a partial evaporation, thus creating a mixture of liquid and vapor with lower pressure and temperature (Evaporation Pressure and Temperature). This vapour-liquid mixture moves through the evaporator, absorbing the heat from a source which it is desired to cool and can be exchanged directly or indirectly through a secondary circuit, completely evaporating the mixture. The refrigerant, again saturated or superheated vapor, returns to the compressor to complete the cycle. The described cycle is based on the ideal cycle, where it is assumed: isentropic compression; isenthalpic expansion; no loss of load in the circuit. In practice, other components are installed in the cycle, the most common being: liquid accumulator, oil separator, liquid distributor, among others. It should be borne in mind that a refrigeration cycle is a thermal system that transfers energy in the form of heat from a region of low energy potential to a region of high energy potential. The result of this transfer is a positive balance of energy variation, meaning that energy enters the system (work supplied to the compressor), thus an external source of energy is required in a refrigeration cycle. The performance of a refrigeration cycle is usually measured using the Coefficient of Performance (COP), defined by the ratio between the refrigeration rate and the compressor work, Equation 1. .(S.; COSTA; C., 2013).

$$COP = \frac{\dot{Q}_{evap}}{\dot{W}_{comp}} \tag{1}$$

2.2 MATHEMATICAL MODEL

The mathematical model consists of an energy balance in each of the components shown in figure 1, taking into account the premises of item 2.1. The set of equations that make up the model are able to describe the behavior of the cycle, allowing to simulate different operating conditions in a practical, fast and low cost way.

EVAPORATOR SIZING

An extension of Newton's law of cooling with the overall heat exchange coefficient, U, a temperature difference, DTML varying with position in the heat exchanger, can be used to determine the area of a double tube heat exchanger, according to equation 2.

$$S_{evap} = \frac{\dot{Q}_{evap}}{U\ DTML} \tag{2}$$

where: U is the overall heat exchange coefficient, (kJ/m2K); DTML is the logarithmic temperature difference, K.
The DTML can be calculated using equation 3:

$$DTML = \frac{(T_{H\ in} - T_{C\ in}) - (T_{H\ out} - T_{C\ out})}{\ln\left(\frac{(T_{H\ in} - T_{C\ in})}{(T_{H\ out} - T_{C\ out})}\right)} \tag{3}$$

where: $T_{H\ in}\ e\ T_{H\ out}$ are the inlet and outlet temperatures of the hot fluid, K; $T_{C\ in}\ e\ T_{C\ out}$ are the inlet and outlet temperatures of the cold fluid, K.

The overall heat exchange coefficient, U is given by equation 4:

$$U = \frac{1}{\frac{1}{\alpha_H} + \frac{1}{\alpha_C}} \tag{4}$$

where: $\alpha_H\ e\ \alpha_C$ are the convective heat exchange coefficients of the hot and cold fluid respectively, (kJ/m2K).

Considering the flow of the hot fluid as internal and single-phase, the heat exchange coefficient of the hot fluid can be determined by the Dittus-Boelter correlation expressed in equation 5:

$$\alpha_H = \frac{(0.023\ Re^{0.8}\ Pr^{0,3})\ k}{\mathrm{D}} \tag{5}$$

where: Re is the dimensionless Reynolds number; Pr is the Prandtl number, dimensionless; D is the tube diameter, m; k is the thermal conductivity of the fluid, (W/mK).

Considering the cold fluid flow as two-phase evaporation, the heat exchange coefficient can be determined by the DENGLER correlation; ADDOMS, (1956) expressed in equation 6. The heat exchange coefficient varies with the title

of the liquid-vapor mixture, which in turn varies with the position along the tube, thus an average value was calculated and used for the entire tube.

$$\alpha_c = 3.5 \left(\frac{1}{c}\right)^{0,5} \alpha_{liq} \quad (6)$$

where: c is the Martinelli parameter expressed in equation 7:

$$c = \left(\frac{(1-x)}{x}\right)^{0,9} \left(\frac{\rho_v}{\rho_l}\right)^{0,5} \left(\frac{\mu_l}{\mu_v}\right)^{0,1} \quad (7)$$

where: x is the vapor fraction of the fluid, dimensionless; ρ_v *e* ρ_l are the vapor and liquid densities, (kg/m³); μ_v *e* μ_l are the dynamic, vapor and liquid viscosities (kg/ms).

α_{liq} is expressed in equation 8:

$$\alpha_{liq} = \frac{\left(0.023\ Re_l^{0.8}\ Pr_l^{0,4}\right) k_l}{D} \quad (8)$$

where: Pr_l is the Prandtl number of the liquid, dimensionless; Re_l is the Reynolds number of the liquid expressed in equation 9:

$$Re_l = \frac{G\ (1 - X)\ D}{\mu_l} \quad (9)$$

G is the mass velocity, [(kg/s) /m2], and can be calculated according to equation 10:

$$G = \frac{\dot{m}}{A} \quad (10)$$

where: $\dot{m}$ is the mass flow rate of the fluid, (kg/s); A is the cross-sectional area of the tube, m².

Isentropic compressor efficiency:

The isentropic efficiency of the compressor is defined by equation 11:

$$n_{isentrópica} = \frac{\dot{W}_{comp\ iso}}{\dot{W}_{comp\ real}} \quad (11)$$

where: $\dot{W}_{comp\ real}$ is the actual compressor work done on the working fluid given in W and which can be calculated by equation 12
:

$$\dot{W}_{comp\ real} = \dot{m}_{fluido}(\ h_{comp\ out\ real} - h_{comp\ in}) \quad (12)$$

where: $h_{comp\ in}$ is the enthalpy of the fluid at the evaporating pressure and at the superheating temperature, (kJ/kg); $h_{comp\ out}$ is the enthalpy of the fluid at the condensing pressure and at the actual compressor discharge temperature, (kJ/kg) obtained through the measurements carried out by (SÁNCHEZ *et al.*, 2017).

The experimental data and the calculated isentropic work values allowed the creation of a cloud of points, with which it was possible to determine, through linear regression, an expression that allows estimating the isentropic efficiency of the compressor as a function of the compression ratio (γ) defined by equation 13:

$$\gamma = \frac{P_{evap}}{P_{cond}} \quad (13)$$

where: P_{evap} is the evaporating pressure, kPa; P_{cond} is the condensing pressure, kPa;

The isentropic efficiency can be calculated using equation 14:

$$n_{isentrópica} = -111.62\ \gamma^4 + 135.7\ \gamma^3 - 58.761\ \gamma^2 + 9.759\ \gamma + 0.0901 \quad (14)$$

With this, it is possible to calculate the actual work of the compressor according to equation 15:

$$\dot{W}_{comp\ real} = \frac{\dot{W}_{comp\ iso}}{n_{isentrópica}} \quad (15)$$

With the real work of the compressor, we can calculate the real enthalpy of the fluid at the compressor outlet through equation 16
:

$$h_{comp\ out\ real} = \frac{\dot{W}_{comp\ real}}{\dot{m}_{fluido}} + h_{comp\ in} \quad (16)$$

Thus the actual compressor discharge temperature can be determined as the temperature corresponding to the condensing pressure and the actual enthalpy at the compressor outlet.

Overall compressor efficiency:

The overall efficiency of the compressor is defined by equation 17:

$$n_{global} = \frac{\dot{W}_{comp\ iso}}{\dot{W}_{eletrico}} \quad (17)$$

where: $\dot{W}_{eletrico}$ is the electrical power consumed by the compressor measured experimentally, W.

Like the isentropic efficiency, the experimental values of electrical power measured by (SÁNCHEZ *et al*., 2017) and the calculated isentropic work values allowed the creation of a cloud of points with which it was possible to determine, through linear regression, an expression that allows estimating the global efficiency of the compressor as a function of the compression ratio (γ) defined by equation 18:

$$n_{global} = -125.71\,\gamma^4 + 159.57\,\gamma^3 - 74.189\,\gamma^2 + 14.589\,\gamma - 0.6567 \quad (18)$$

Mechanical efficiency of the compressor:

The mechanical efficiency of the compressor is given by equation 19:

$$n_{mecanica} = \frac{n_{global}}{n_{isentrópica}} \quad (19)$$

CONDENSER SIZING

As with the evaporator, Newton's cooling law can also be used to determine the area of the condenser, equations 6 to 8.

In the condenser, α_H is determined considering the flow as a two-phase condensation, thus the heat exchange coefficient can be determined by the CHATO correlation, (1962) expressed in equation 20. The heat exchange coefficient varies with the wall temperature , which varies along the heat exchanger tube, so an average value for the entire tube was used.

$$\alpha_H = \left(\frac{0.55\,(g\,\rho_l\,(\rho_l - \rho_v)\,{k_l}^3 h'_{lv}}{\mu_l\,(T_{cond} - T_p)\,D}\right)^{0,25} \quad (20)$$

where: g is the acceleration due to gravity, (m/s²); $T_{cond}\ e\ T_p$ are the condensing temperatures of the fluid and the tube wall, K; h'_{lv} is the heat of vaporization of the modified fluid given by equation 21, (kJ/kg):

$$h'_{lv} = h_{lv} + 0.375\,C_{pl}(T_{cond} - T_p) \quad (21)$$

where: h_{lv} is the heat of vaporization of the fluid, (kJ/kg); C_{pl} is the specific heat of the fluid at constant pressure, (kJ/kg).

The tube wall temperature can be expressed by equation 22:

$$T_p = \frac{T_{cond}\,\alpha_H + T_c\,\alpha_H}{\alpha_H + \alpha_C} \quad (22)$$

As observed in equations 20 and 21, the tube wall temperature and the heat exchange coefficient are dependent on each other, so it is necessary to use an iterative process to calculate the wall temperature. In this process, initially the wall temperature is arbitrated as the average temperature of the secondary and primary fluids of the condenser. Thus, the value of the heat exchange coefficient and the temperature of the wall is calculated, which is updated, repeating the process until there is convergence.

2.3 OPTIMIZATION

According to ANDRADE, (2014) the optimization of a process or system consists of obtaining the best solution for the process considering certain restrictions, using specific methods.

To quantify the best solution obtained in the optimization process, it is necessary to define an objective function f(x), which must be maximized or minimized, according to the need of the problem. This optimization is subject to h(x) equality constraints and/or g(x) inequality constraints. The final result of the objective function is determined by manipulating adjustable (or manipulated) variables, which may physically represent the size of the equipment or operating conditions (ANDRADE, 2014).

To optimize the problem, a genetic-type global optimization algorithm was used whose objective function can be described by equation 23:

$$f(x) = \max\left(COP_{global}\right) \tag{23}$$

where: x is the vector of manipulated variables composed by the condensation pressure and the refrigerant fluid;

The inequality constraints are defined by equations 24 to 29:

$$g_1(x) = T_{cond} \geq T_{ambiente}\ (25°C) \tag{24}$$
$$g_2(x) = S_{evap} \leq 12\ m^2 \tag{25}$$
$$g_3(x) = S_{cond} \leq 12\ m^2 \tag{26}$$
$$g_4(x) = 1500W \tag{27}$$
$$g_5(x) = Q_{cond} \leq 1500W \tag{28}$$
$$g_6(x) = \dot{W}_{eletrico} \geq 0 \tag{29}$$

where S_{evap} represents the area of the evaporator, m^2; S_{cond} is the area of the condenser, m^2; Q_{evap} is the maximum heat exchanged in the evaporator,W; Q_{cond} is the maximum heat exchanged in the condenser.

2.4 CALCULATION METHODOLOGY

The mathematical model developed has as optimization parameters the refrigerant fluid, the condensing pressure and the COP of the system. For this, the condensing temperature, degree of superheating and undercooling and the thermal load of the evaporator are provided as input parameters. Through these data, an energy balance is carried out in the expansion device and in the evaporator, which is dimensioned. Subsequently, the isentropic work of the compressor and the mechanical, isentropic and global efficiencies are calculated in order to obtain the real work and the electrical power of the compressor. Finally, an energy balance is carried out in the condenser for later dimensioning and in this way the COP of the system is calculated.

3. RESULTS

3.1 MODEL VALIDATION

The model was validated through the results obtained experimentally by (SÁNCHEZ *et al*., 2017). Table 1 shows the results of the simulations performed to validate the model. The accuracy of the model was determined according to equation 30:

$$E_{modelo} = \left|\frac{COP_{experimental} - COP_{global}}{COP_{experimental}}\ 100\right| \tag{30}$$

Table 1 - Simulation results

Fluido	Carga Térmica [W]	Temperatura de evaporação[C]	Grau de super-	Temperatura de	Grau de sub -	COP experimental [-]	COP simulado [-]	Erro do modelo

			aquecimento [C]	condensação [C]	resfriamento [C]			
R134a	630.31	-10.23	11.09	24.66	3.85	2.08	2.20	6%
	493.93	-9.93	11.67	44.50	3.76	1.54	1.36	11%
	1.030.67	0.09	11.09	25.35	4.74	2.88	2.81	2%
	951.57	0.57	12.61	34.99	4.61	2.47	2.23	10%
R152A	611.12	-9.82	11.48	25.24	2.70	2.17	2.19	1%
	953.49	0.24	9.76	25.11	2.05	3	2.76	8%
	858.30	0.15	9.65	35.33	2.08	2.5	2.17	13%
R1234yf	599.74	-9.71	9.28	24.98	6.37	1.87	2.17	16%
	485.51	-9.56	9.44	45.34	5.81	1.37	1.34	3%
	991.43	0.33	8.53	25.79	6.89	2.57	2.61	2%
	883.08	0.02	9.93	35.13	4.36	2.21	2.10	5%
R1234ze(E)	460.42	-10.23	10.21	24.85	2.86	1.86	2.20	18%
	766.40	0.32	9.07	25.12	1.99	2.63	2.82	7%
	690.74	0.43	8.96	35.22	3.70	2.28	2.21	3%
	633.28	0.46	8.70	45.16	7.71	1.99	1.85	7%
R600a	377.79	-9.42	4.21	25.38	7.15	1.88	2.27	21%
	285.35	-9.70	4.98	44.85	5.17	1.31	1.42	8%
	598.19	0.67	6.04	25.47	5.43	2.69	2.79	4%

Source: Prepared by the author, 2022.

Comparison between simulated results and experimental data showed a mean absolute relative error of 8.16% with a standard deviation of 5.75%. The average COP of the refrigeration cycle was 2.01 with a standard deviation of 0.45.

3.2 CYCLE RESPONSE WITH INCREASE IN CONDENSATION PRESSURE

Figures 3 and 4 show the behavior of the COP, the isentropic efficiency and the mechanical efficiency with the variation of the condensing pressure, keeping constant the evaporation pressure, the thermal load of the evaporator, the degree of superheating and the degree of subcooling.

Figure 3 - COP x Condensation pressure

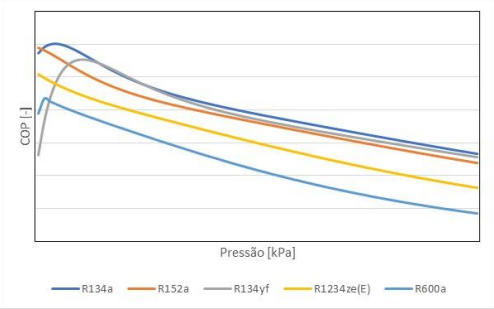

Source: Prepared by the author, 2022

Figure 4 - Isentropic efficiency x Condensing pressure

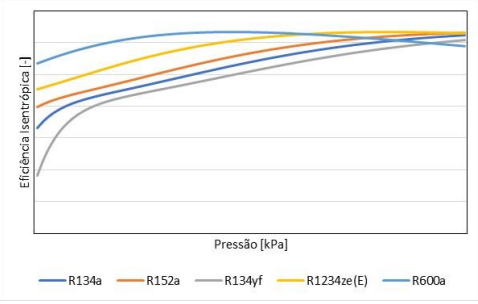

Source: Prepared by the author, 2022.

3.3 OPTIMIZATION

Two types of optimization were performed. The first consists of a constrained nonlinear programming optimization algorithm. This was carried out to find the optimum operating pressure for all the operating conditions in Table 1. The second consists of a constrained genetic-type global optimization algorithm. This was used in order to determine the optimal fluid and pressure for four conditions in Table 1: Conditions of lower and higher COP and lower and higher thermal load on the evaporator.

The lower limit of optimization was defined as 200 kPa above the evaporation pressure and the upper limit being 1200 kPa, referring to the highest pressure of the experimental data. The initial estimate was defined as the lower limit of the search.

For the first type of optimization, MATLAB's fmincon function was used. The objective function and restrictions were defined in equations 23 to 29. In this case, the manipulated variable was the condensation pressure. The results of the optimizations can be seen in Table 2:

Table 2 - Result of Optimization of Simulated Values

Fluido	Carga térmica do evaporador [W]	Pressão de Cond. [kPa]	COP [-]	Pressão de Cond. otimizada [kPa]	COP otimizado [-]	Ganho
R134a	630.31	658.67	2.20	547.71	2.47	10.94%
	493.93	1.144.95	1.36	57.,7	2.5	45.43%
	1.030.67	672.35	2.81	657.5	2.82	0.28%
	951.57	886.73	2.23	667.23	2.81	20.71%
R152A	611.12	600.67	2.19	512.9	2.5	12.45%
	953.49	598.36	2.76	596.1	2.75	-0.21%
	858.30	801.11	2.17	594.45	2.75	21.03%
R1234yf	599.74	682.20	2.17	591.72	2.5	13.19%
	485.51	1.163.51	1.34	591.72	2.5	46.59%
	991.43	697.84	2.61	708.47	2.62	0.29%
	883.08	898.26	2.10	702.29	2.57	18.41%
R1234ze(E)	460.42	496.19	2.20	450	2.37	7.35%
	766.40	500.26	2.82	490.25	2.82	0.09%
	690.74	671.46	2.21	492.25	2.86	22.83%
	633.28	879.72	1.85	492.15	2.95	37.33%
R600a	377.79	354.58	2.27	350.00	2.29	0.76%
	285.35	602.15	1.42	350.00	2.24	36.72%
	598.19	355.51	2.79	360.75	2.79	0.10%

Source: Prepared by the author, 2022.

The results of the optimization of the simulated conditions showed an average COP of 2.59 with a standard deviation of 0.19, representing an efficiency gain of 22% in relation to the initial conditions (COP increase from 2.01 to 2.59) . This increase in COP is greater than the uncertainty of the model (8.16%), so we can conclude that the optimization of the condensing pressure brought a real and significant gain.

For the global optimization, a genetic-type algorithm was used in order to identify the fluid and the condensation pressure that maximizes the COP. The results are in table 3:

Table 3 - Optimization Results - Optimized Pressure and Fluids

Fluido	Carga térmica do evaporador [W]	Pressão de Cond. [kPa]	COP [-]	Fluido Otimizado	Pressão de Cond. Otimizada [kPa]	COP Otimizado [-]
R152a	1.030.67	672.35	2.81	R134a	660.96	2.82
R600a	285.35	602.15	1.42	R134a	457.48	3.02
R1234ze(E)	766.40	500.26	2.82	R134a	460.14	3.03
R1234yf	485.51	1.163.51	1.34	R134a	660.07	2.75

Source: Prepared by the author, 2022.

The optimization results seeking to find an optimum fluid and pressure showed an average COP of 2.92, with a standard deviation of 0.12, representing an efficiency gain of 32% compared to the initial conditions (COP increase of 2.01 to 2.92) and 11% compared to the optimized pressure (COP increase from 2.59 to 2.92). It can be concluded that both the condensing pressure and the working fluid have a significant impact on the energy efficiency of the cycle.

In order to analyze which fluid is the best option to replace R134a in the refrigeration cycle, the same operating conditions in table 3 were optimized without R134a as an option. The results are in table 4:

Table 4 - Optimization result for selecting the replacement fluid for R134a

Fluido	Carga térmica do evaporador [W]	Pressão de Cond. [kPa]	COP [-]	Fluido Otimizado	Pressão de Cond. Otimizada [kPa]	COP Otimizado
R152a	1.030.67	672.35	2.81	R152a	601.15	2.8
R600a	285.35	602.15	1.42	R152a	455.2	2.88
R1234ze(E)	766.40	500.26	2.82	R152a	645.56	2.67
R1234yf	485.51	1.163.51	1.34	R152a	506.77	2.77

Source: Prepared by the author, 2022.

The optimization results seeking to find the fluid that best replaces R134a from the point of view of energy efficiency showed an average COP of 2.78 and standard deviation of 0.09. In relation to R134a, R152a was 5% less efficient (COP reduction from 2.92 to 2.78) and R152a was 28% more efficient than the original cycle conditions (COP increase from 2.01 to 2.78). 2.78) and 7% more efficient than the condition where only the pressure was optimized (COP increase from 2.59 to 2.78). It can be concluded that it is possible to replace R134a without losing cooling capacity and still increasing the efficiency of the cycle..

4. CONCLUSION

Analysis of the graph in Figure 3 showed that the COP is directly proportional to the condensing pressure for a constant evaporating pressure. The graph in figure 4 shows that for a constant evaporating pressure, the isentropic efficiency increases with the condensing pressure. The mechanical efficiency (graph in figure 5), on the other hand, behaves inversely proportional to the condensing pressure, and for a low compression ratio the mechanical efficiency is also low. Thus, for a refrigeration cycle, the optimal condensing pressure is the one whose mechanical and isentropic efficiency have the maximum value between them.

Model validation (Table 1) showed a mean absolute relative error of 8.16% with a standard deviation of 5.75%. The average COP of the refrigeration cycle was 2.01 with a standard deviation of 0.45.

The optimization of the condensing pressure (Table 2) resulted in an average COP of 2.59 with a standard deviation of 0.19, representing an efficiency gain of 22% (COP increase from 2.01 to 2.59). This result is consistent with the result obtained by ANDRADE, (2014) who achieved an efficiency increase of 32% (COP increase from 1.69 to 2.5) by varying the condensation pressure.

Optimization of pressure and refrigerant (Table 3) showed that R134a is the fluid that presents the best performance from an energy point of view, with an average COP of 2.92, with a standard deviation of 0.12, representing a gain efficiency of 32% in relation to the initial conditions (COP increase from 2.01 to 2.92) and 11% in relation to the optimized pressure (COP increase from 2.59 to 2.92).

The optimization for choosing the fluid that best replaces R134a (Table 4) from the point of view of energy efficiency was R152a, with an average COP of 2.78 and standard deviation of 0.09. In relation to R134a, R152a was 5% less efficient (COP reduction from 2.92 to 2.78) and R152a was 28% more efficient than the original cycle conditions (COP increase from 2.01 to 2.78). 2.78) and 7% more efficient than the condition where only the pressure was optimized (COP increase from 2.59 to 2.78). This result is consistent with those obtained by SÁNCHEZ *et al*.,(2017) who found experimentally that the most suitable fluids to replace R134a are R134yf and R152a. The results of this work corroborate those obtained by SÁNCHEZ *et al.*, (2017) and demonstrate that from the point of view of energy efficiency, R152a is more suitable than R123yf to replace R134a.

The mathematical model developed in this work proved to be a robust tool capable of optimizing the operating conditions of a refrigeration cycle in order to increase energy efficiency. Comparing with other works, the results were consistent, and the methodology adopted also allows the study and optimization of isentropic and mechanical efficiency in a simplified way and at low cost. The results showed that if the refrigeration system is well adjusted, it is possible to retrofit it without loss of cooling capacity or energy efficiency.

5. REFERENCES

ANDRADE, T. A. Optimization of refrigeration cycles for the production of liquefied natural gas. 2014. 150 f. State University of Campinas, 2014.
BAAKEEM, S.S.; ORFI, J.; ALABDULKAREM, A. Optimization of a multistage vapor-compression refrigeration system for various refrigerants. Applied Thermal Engineering, v. 136, p. 84–96, 25 May 2018. Available at: <https://www.sciencedirect.com/science/article/pii/S1359431117367947>. Accessed on: 7 Jul. 2018.
BELMAN-FLORES, J. M. *et al*. Experimental study of R1234yf as a drop-in replacement for R134a in a domestic refrigerator. International Journal of Refrigeration, vol. 81, p. 1–11, 1 set. 2017. Available at: <https://www.sciencedirect.com/science/article/pii/S0140700717301925>. Accessed on: 5 Jul. 2018.
BOLAJI, B. O. Experimental study of R152a and R32 to replace R134a in a domestic refrigerator. Energy, v. 35, no. 9, p. 3793–3798, 1 set. 2010. Available at: <https://www.sciencedirect.com/science/article/pii/S0360544210003014>. Accessed on: 6 Jul. 2018.
CABELLO, R. *et al*. Energy evaluation of R152a as drop in replacement for R134a in cascade refrigeration plants. Applied Thermal Engineering, v. 110, p. 972–984, 5 Jan. 2017. Available at: <https://www.sciencedirect.com/science/article/pii/S1359431116316064>. Accessed on: 6 Jul. 2018.
CABELLO, R. *et al*. Experimental comparison between R152a and R134a working in a refrigeration facility equipped with a hermetic compressor. International Journal of Refrigeration, vol. 60, p. 92–105, 1 Dec. 2015. Available at: <https://www.sciencedirect.com/science/article/pii/S0140700715001905>. Accessed on: 5 Jul. 2018.
CASTRO, F. S. D. C.; NEVES, C. P. Study on the influence of condensing pressure on the performance of refrigeration cycles. 2014. 1-21 f. University of Rio Verde, 2014.
CHATO, J. C. Laminar Condensation Inside Horizontal and Inclined Tubes. ASHRAE Journal, vol. 4, p. 52–60, 1962.
DENGLER, C.E.; ADDOMS, J. Heat transfer mechanism for vaporization of water in a vertical tube. chem. Engineering Progress Symposium Series, v. 53, no. 18, p. 95–103, 1956.
JOYBARI, M. M. *et al*. Exergy analysis and optimization of R600a as a replacement of R134a in a domestic refrigerator system. International Journal of Refrigeration, vol. 36, no. 4, p. 1233–1242, 1 jun. 2013. Available at: <https://www.sciencedirect.com/science/article/pii/S0140700713000352>. Accessed on: 6 Jul. 2018.
JUAN JOSE GARCIA PABON. EXPERIMENTAL STUDY OF PRESSURE LOSS IN CONVENTIONAL CHANNELS WITH REFRIGERANT R1234yf IN CONVECTIVE BOILING. 2018. 82 f. UFMG, 2018.
MOTA-BABILONI, A. et al. A review of refrigerant R1234ze(E) recent investigations. Applied Thermal Engineering, v. 95, p. 211–222, 25 Feb. 2016.
S., G.F.; COSTA, A.O.S.; C., J. E. F. REFRIGERATION CYCLES: EFFICIENCY CONCEPTS AND STUDIES. . [s.l: s.n.]. , 2013
SÁNCHEZ, D. *et al*. Energy assessment of an R134a refrigeration plant upgraded to an indirect system using R152a and R1234ze(E) as refrigerants. Applied Thermal Engineering, v. 139, p. 121–134, 5 Jul. 2018. Available at: <https://www.sciencedirect.com/science/article/pii/S1359431117380316>. Accessed on: 6 Jul. 2018.
SÁNCHEZ, D. *et al*. Energy performance evaluation of R1234yf, R1234ze(E), R600a, R290 and R152a as low-GWP R134a alternatives. International Journal of Refrigeration, vol. 74, p. 269–282, 1 Feb. 2017. Available at: <https://www.sciencedirect.com/science/article/pii/S0140700716303012>. Accessed on: 29 Jun. 2018.
SILVA, M. V. L. R. Dynamic Simulation of a Refrigeration Cycle for Energy Comparison of Flammable Refrigerants. 2015. Federal University of Rio de Janeiro, 2015.
SHYAM, A.; AKHILESH, A.; B.B.Arora. ENERGY AND EXERGY INVESTIGATIONS OF R1234yf AND R1234ze AS R134a REPLACEMENTS IN MECHANICALLY SUBCOOLED VAPOUR COMPRESSION REFRIGERATION CYCLE. Journal of Thermal Engineering, v. 7, p. 109-132, January, 2021.

6. DISCLAIMER OF LIABILITY

Thiago Pereira Silva and the other authors are solely responsible for the material printed in this work.